Resistive switching characteristics of Ti/ZrO_2/Pt RRAM device*

Lei Xiao-Yi(雷晓艺)[a], Liu Hong-Xia(刘红侠)[a)†], Gao Hai-Xia(高海霞)[a], Yang Ha-Ni(杨哈妮)[b], Wang Guo-Ming(王国明)[c)d)], Long Shi-Bing(龙世兵)[c)], Ma Xiao-Hua(马晓华)[a)b)], and Liu Ming(刘 明)[c)]

[a)] *Key Laboratory of Wide Bandgap Semiconductor Materials and Devices, School of Microelectronics, Xidian University, Xi'an* 710071, *China*
[b)] *School of Advanced Materials and Nanotechnology, Xidian University, Xi'an* 710071, *China*
[c)] *Laboratory of Nano-fabrication and Novel Devices Integrated Technology, Institute of Microelectronics, Chinese Academy of Sciences, Beijing* 100029, *China*
[d)] *Tianjin Key Laboratory of Film Electronic and Communication Devices, Tianjin University of Technology, Tianjin* 300384, *China*

(Received 25 March 2014; revised manuscript received 30 May 2014; published online 24 September 2014)

In this paper, the bipolar resistive switching characteristic is reported in Ti/ZrO_2/Pt resistive switching memory devices. The dominant mechanism of resistive switching is the formation and rupture of the conductive filament composed of oxygen vacancies. The conduction mechanisms for low and high resistance states are dominated by the ohmic conduction and the trap-controlled space charge limited current (SCLC) mechanism, respectively. The effect of a set compliance current on the switching parameters is also studied: the low resistance and reset current are linearly dependent on the set compliance current in the log–log scale coordinate; and the set and reset voltage increase slightly with the increase of the set compliance current. A series circuit model is proposed to explain the effect of the set compliance current on the resistive switching behaviors.

Keywords: resistive random access memory (RRAM), resistive switching (RS), conductive filament (CF), compliance current

PACS: 73.40.Rw, 77.80.Fm, 72.20.–i **DOI:** 10.1088/1674-1056/23/11/117305

1. Introduction

Resistive random access memory (RRAM) is one of the most competitive candidates for the next-generation non-volatile memory (NVM) application due to its simple metal–insulator–metal (M–I–M) structure, fast switching speed, great scalability, and high density integration.[1–6] A larger variety of insulator materials seem to be applicable for the RRAM switching layer (SL), including perovskite oxides,[7] ferromagnetic materials,[8–10] organic materials,[11] solid electrolyte materials,[5,12] and binary transition metal oxides.[13–16] Owing to its superb compatibility with COMS technology, simple constituents, and easy fabrication process, RRAM based on binary transition metal oxide has been intensively investigated. The resistive switching (RS) behavior is generally attributed to the formation and rupture of the conductive filament (CF).[17–19] The compliance current (I_{comp}) in the set process has a great effect on the RS behavior.[1] However, full understandings of the switching mechanisms and particular effects of the compliance current on the RS behaviors still need further exploration.

In this paper, we examine the Ti/ZrO_2/Pt resistive switching memory devices. The RS mechanism and current conduction mechanism have been investigated respectively. In addition, different RS behaviors at different magnitudes of compliance current during the set process have been observed. The relationships between the switching parameters and I_{comp} are obtained, and a series circuit model has been used to explain the phenomenon in the Ti/ZrO_2/Pt RRAM device.

2. Experimental details

ZrO_2-based RRAM devices with Pt/Ti top electrodes (TE) are fabricated on Pt/Ti/SiO_2/Si substrates as shown in Fig. 1. The Pt layer in TE is used to avoid the oxidation of the Ti electrode, and the Ti layer in the bottom electrode (BE) is deposited as an adhesion layer. The thickness of ZrO_2 film is 20 nm, and the area of the device is 100×100 μm^2. All electrical characterizations of the RRAM devices are measured by

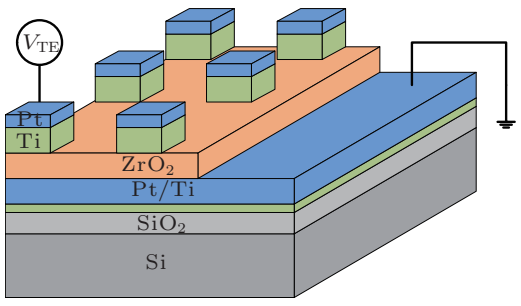


Fig. 1. (color online) Schematic structure of the Ti/ZrO_2/Pt RRAM device.

*Project supported by the National Basic Research Program of China (Grant No. 2011CBA00606), the National Natural Science Foundation of China (Grant Nos. 61106106, 11304237, 61376099, and 11235008), and the Specialized Research Fund for the Doctoral Program of Higher Education of China (Grant Nos. 20130203130002 and 20110203110012).

†Corresponding author. E-mail: hxliu@mail.xidian.edu.cn

© 2014 Chinese Physical Society and IOP Publishing Ltd

an Agilent B1500A high-precision semiconductor parameter analyzer with biasing at the TE and grounding at the BE at ambient temperature.

3. Results and discussion

Figure 2 shows the typical bipolar RS *I*–*V* curve of the Ti/ZrO_2/Ti device. Firstly, using the direct current (DC) voltage sweep mode with a current compliance of 5 mA, a sudden increase of current occurs at 3.665 V, which is called the forming process, as shown in the inset of Fig. 2. After the forming process, the conduction path connecting the top and bottom electrodes is formed and the device reaches a low resistance state (LRS). By sweeping a negative voltage from 0 V to −1 V, the device is switched from the LRS to the high resistance state (HRS) at about −0.48 V, known as the reset process. Subsequently, the device switches back to the LRS through a set process by sweeping the voltage from zero upward with a current compliance of 5 mA.

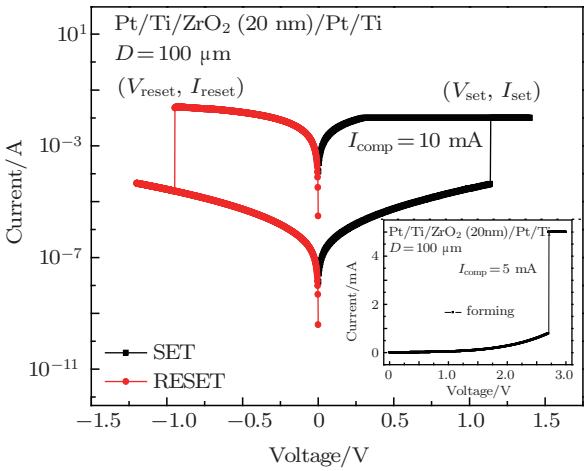


Fig. 2. (color online) Typical resistive switching *I*–*V* curves of Ti/ZrO_2/Pt.

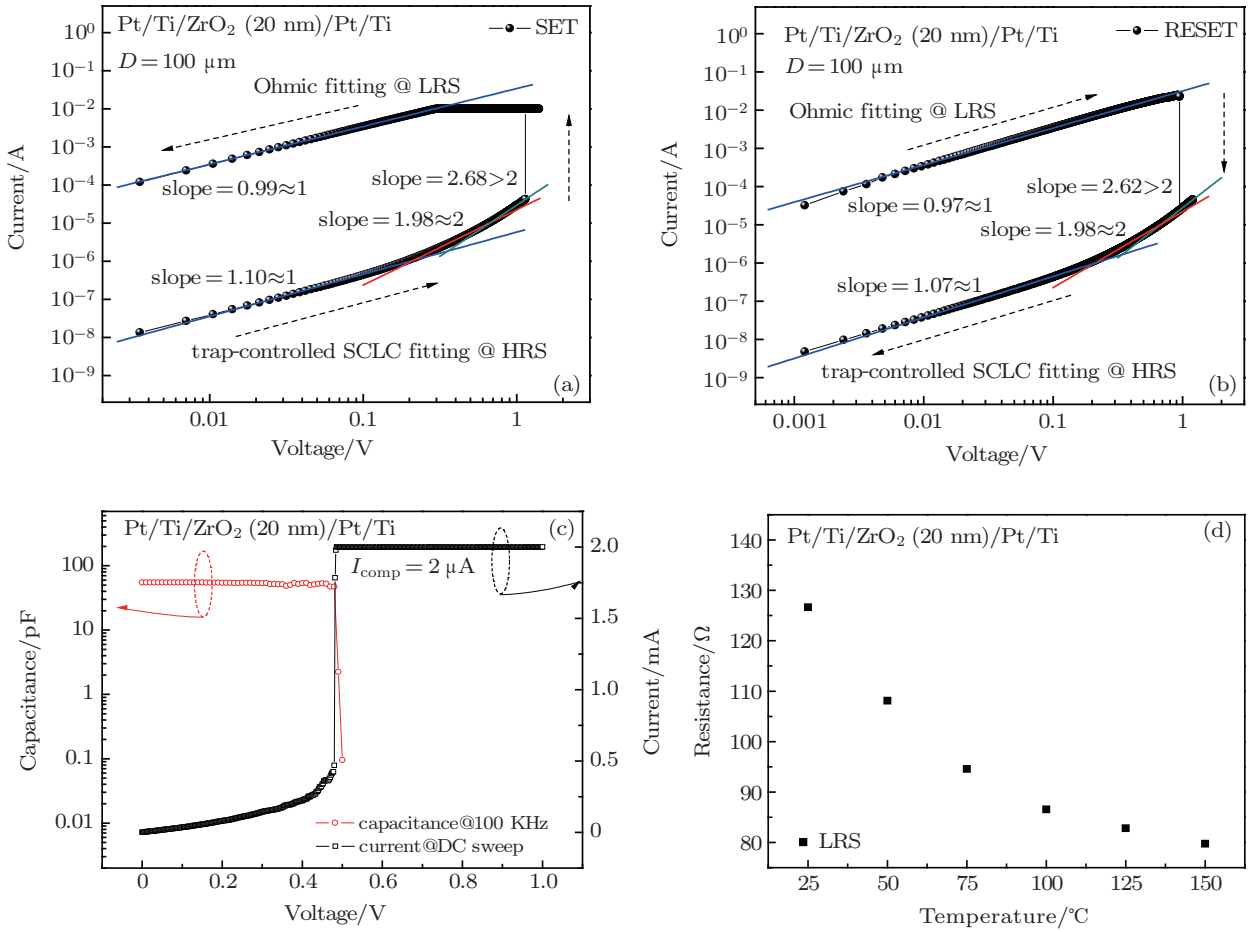


Fig. 3. (color online) Linear fitting for the *I*–*V* curves using double logarithmic coordinates during (a) the set process and (b) the reset process. (c) Capacitance characteristic of the device and (d) resistance versus temperature for LRS.

In order to investigate the conduction mechanism of the Ti/ZrO_2/Pt cell, the *I*–*V* curves during set and reset processes are analyzed in double logarithmic coordinates in Figs. 3(a) and 3(b). Both figures in LRS exhibit the linear dependence with a slope of ∼ 1 and indicate that ohmic conduction behavior is dominant. However, the *I*–*V* characteristic of HRS

exhibits a complex shape. As described in Fig. 3, the current in HRS is governed by the trap-controlled space charge limited current (SCLC),[20–22] which is divided into three regions in double logarithmic coordinates as follows:

(i) the linear ohmic conduction (i.e., $I \propto V$) in the low voltage region;

(ii) the followed $I \propto V^2$ square region;

(iii) the steep increase in current in the high voltage region.

It is noticed that the resistance at LRS is independent of the polarity of applied voltage (see Figs. 3(a) and 3(b)). It suggests that the resistive switching cannot attribute to the Schottky barrier at the metal/dielectric interface, but the traps inside the dielectric itself. Moreover, for Schottky barrier type RRAM, both HRS and LRS have a capacitive nature. In contrast, it has different characteristics in filamentary type RRAM: a capacitive element dominates the HRS and an inductor dominates the LRS.[23] As shown in Fig. 3(c), the device switches from HRS to LRS, and the capacitance changes from positive to negative. In addition, the resistance at LRS decreases with increasing temperature, as shown in Fig. 3(d). This result means that the conduction path is composed of oxygen vacancies rather than metal atoms.

The switching process of the Ti/ZrO_2/Pt RRAM device is schematically shown in Fig. 4. During the forming process, the electrons can obtain enough energy from the applied electric field to rupture the Zr–O bonds. The oxygen ions (O^{2-}) are driven by the electric field and absorbed by the Ti top electrode, which is like the oxygen reservoir.[3] As a result, the CF composed of the oxygen vacancies is formed. Then electrons can transport through the CF and the device obtains the LRS (see Fig. 4(a)). Subsequently, the oxygen ions migrate from Ti electrode to SL due to the opposite electric field during the reset process, and then recombine with the oxygen vacancies,[24] as described in Fig. 4(b). The CF is ruptured and the HRS is obtained. Because the oxygen vacancies are produced after the forming process, the Schottky barrier of the pristine state is modified and the energy band diagram is changed as shown in Fig. 4(c). Therefore, the conduction mechanism at HRS is SCLC.[25] By applying positive voltage, the device can be set again to LRS. This set/reset switching behavior is repeatable by the cyclical operation of the positive/negative voltage.

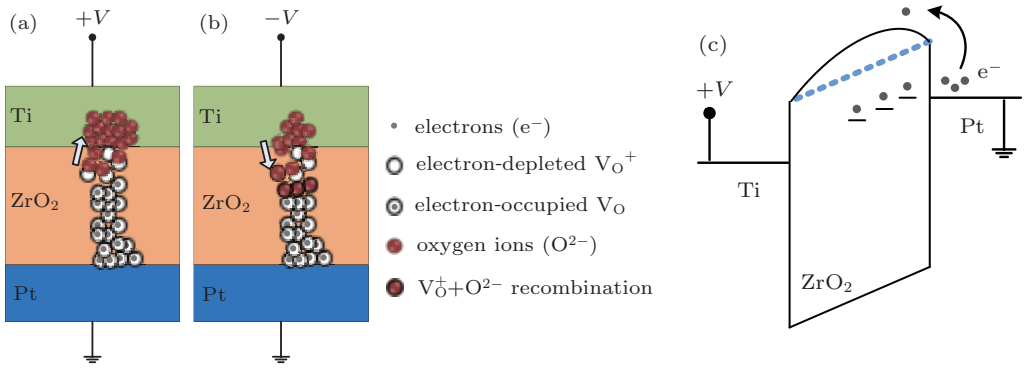


Fig. 4. (color online) Schematics showing (a) the formation of CF at LRS and (b) the rupture of CF during HRS. (c) SCLC conduction energy band diagram.

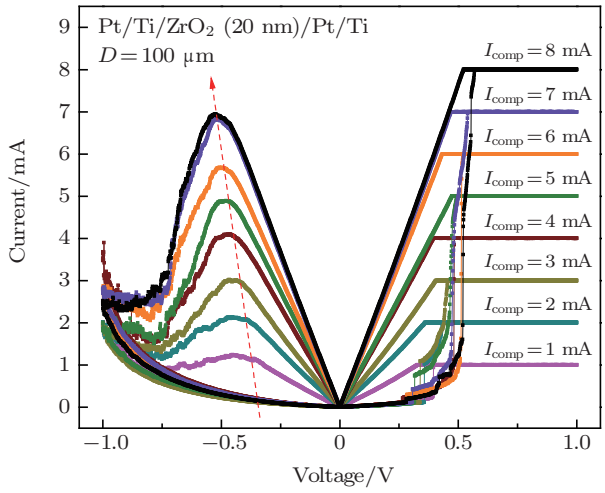


Fig. 5. (color online) RS I–V curves of Ti/ZrO_2/Ti device for different I_{comp}.

In every switching cycle, the current compliance during the set process is essential to prevent permanent damage of the RRAM devices and it is an important factor which influences the RS behavior. Figure 5 shows the switching characteristics of the Ti/ZrO_2/Ti device using different I_{comp}, ranging from 1 mA to 8 mA. It is evident that I_{comp} induced switching performance changes are significant.

Figures 6(a)–6(d) show the dependences of the LRS resistance, the reset current, the set voltage, and the reset voltage on I_{comp}, respectively. As shown, the LRS resistance decreases, while the reset current increases with increasing I_{comp}. In addition, they become linearly dependent on I_{comp} in the log–log scale coordinate. The set voltage and reset voltage increase linearly with the increase in I_{comp}, as shown in Figs. 6(c) and

6(d). From the slopes of fitting lines, the changes of V_{set} and V_{reset} are slighter than LRS resistance and I_{reset}. These results suggest that the Ti/ZrO_2/Ti RRAM device is potentially suitable for multi-level memory application by controlling the magnitude of the compliance current during the set process.

During the set process, depending on the current compliance, trap density varies. When the compliance current is large, more traps are generated. As we know, when the trap density in the dielectric becomes very high, they form a trap sub band, and the barrier between traps gets lowered. At the same time, the free electron concentration increases significantly. The conductance (σ) and electron concentration (n) follow the relationship

$$\sigma = nq\mu_n,$$

where μ_n is the electron mobility. As a result, the conductance increases, which results in a decrease in LRS resistance and an increase in reset current (see Figs. 6(a) and 6(b)). When the compliance current is small, a small number of traps are generated and those traps tend to be isolated from each other. Electrons therefore get localized. The overall effect is a decrease in device conductance.

Finally, an equivalent circuit model of the device is proposed to present a further explication. As shown in Fig. 7, the oxygen vacancies composed of CF, the Ti reservoir, and the Pt electrode can be considered as three resistors in a series, i.e., R_{CF}, R_{TE}, and R_{BE}. In other words, the device resistance is equal to the sum of R_{CF}, R_{TE}, and R_{BE}. In addition, the impact of the formation/rupture of the CF on the TE resistance can be neglected, since the volume of TE is significantly larger compared to that of the filament.

When a lower I_{comp} is applied during the set process, a smaller set voltage is required (see Fig. 6(c)) and the number of oxygen ions absorbed by the Ti top electrode is smaller, resulting in a few vacancies in SL. Therefore, the cross section of CF is smaller[2] and its resistance R_{CF} is larger (see Fig. 6(a)). According to the voltage divider rule in a series circuit (V_{CF}= $[R_{CF}/(R_{CF}+R_{TE}+R_{BE})]V_{TE}$), the voltage crossing R_{CF} is higher for the same bias condition. That is, lower percentage of V_{TE} is applied to the Ti reservoir to drive the reserved oxygen ions back to recombine with oxygen vacancies during the reset process. Additionally, from the slopes in Fig. 6, the changes of V_{reset} are much slighter than I_{reset}. Therefore, a smaller I_{comp} leads to a smaller reset current due to fewer oxygen ions generated and recombined, as shown in Figs. 5 and 6(b). In contrast, larger current compliance requires a larger amount of oxygen ions in the switching process. Consequently, higher V_{set}, V_{reset}, and I_{reset} and lower LRS resistance are obtained, as shown in Fig. 6.

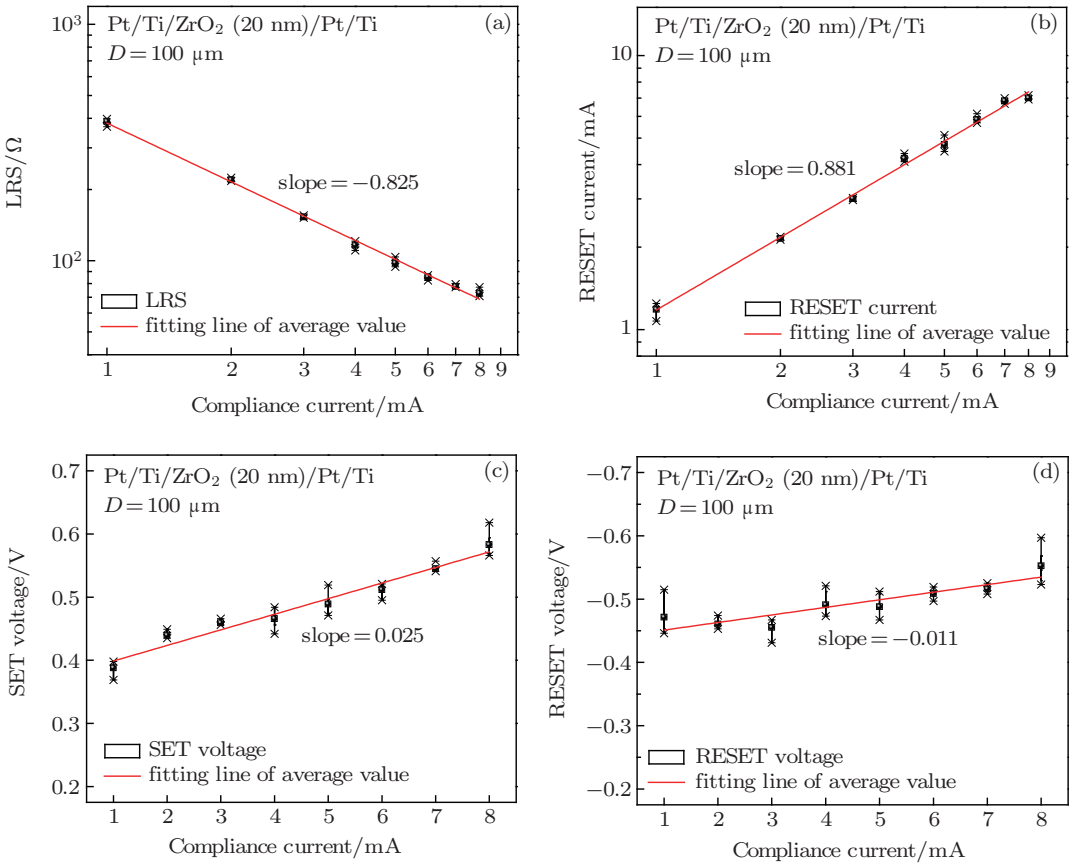


Fig. 6. (color online) Dependence of (a) LRS resistance, (b) reset current, (c) set voltage, and (d) reset voltage on I_{comp}.

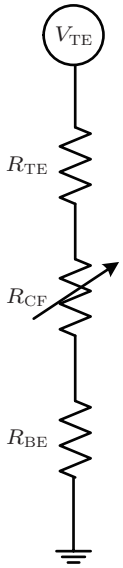


Fig. 7. Schematic of the equivalent circuit model of the device.

4. Conclusion

The bipolar RS characteristics of the Ti/ZrO_2/Ti RRAM device have been demonstrated. The formation and rupture of the CF composed of oxygen vacancies is the dominant mechanism to achieve RS. According to the fitted *I*–*V* curves, the conduction mechanism of LRS is dependent on the ohmic conduction. For the HRS, it is the trap-controlled space charge limited current (SCLC) mechanism. In addition, the compliance current during the set process is an important factor which influences the RS behavior. Since the RS parameters are linearly dependent on the set compliance current, multi-level storage can be achieved by controlling the magnitude of the compliance current during the set process. Finally, the voltage divider rule in a series circuit model is used to explain the observed phenomenon.

References

[1] Li Y T, Long S B, Zhang M H, Liu Q, Shao L B, Zhang S, Wang Y, Zuo Q Y, Liu S and Liu M 2010 *IEEE Electron Dev. Lett.* **31** 117
[2] Puglisi F M, Larcher L, Bersuker G, Padovani A and Pavan P 2013 *IEEE Electron Dev. Lett.* **34** 387
[3] Wong H S P, Lee H Y, Yu S M, Chen Y S, Wu Y, Chen P S, Lee B, Chen F T and Tsai M J 2012 *Proc. IEEE* **100** 1951
[4] Liu M, Abid Z, Wang W, He X L, Liu Q and Guan W H 2009 *Appl. Phys. Lett.* **94** 233106
[5] Sun J, Liu Q, Xie H W, Wu X, Xu F, Xu T, Long S B, Lü H B, Li Y T, Sun L T and Liu M 2013 *Appl. Phys. Lett.* **102** 053502
[6] Chang K C, Tsai T M, Chang T C, Wu H H, Chen J H, Syu Y E, Chang G W, Chu T J, Liu G R, Su Y T, Chen M C, Pan J H, Chen J Y, Tung C W, Huang H C, Tai Y H, Gan D S and Sze S M 2013 *IEEE Electron Dev. Lett.* **34** 399
[7] Liu C Y, Wu P H, Wang A, Jang W Y, Young J C, Chiu K Y and Tseng T Y 2005 *IEEE Electron Dev. Lett.* **26** 351
[8] Zhuang W W, Pan W, Ulrich B D, Lee J J, Stecker L, Burmaster A, Evans D R, Hsu S T, Tajiri M, Shimaoka A, Inoue K, Naka T, Awaya N, Sakiyama K, Wang Y, Liu S Q, Wu N J and Ignatiev A 2002 *IEDM Tech. Dig.* 193
[9] Zhang F, Lin Y B, W H, Miao Q, Gong J J, Chen J P, Wu S J, Zeng M, Gao X S and Liu J M 2014 *Chin. Phys. B* **23** 027702
[10] Garcia V, Fusil S, Bouzehouane K, Enouz-Vedrenne S, Mathur N D, Barthelemy A and Bibes M 2009 *Nature* **460** 81
[11] Tu C H, Kwong D L, Lee D and Lai Y S 2006 *Appl. Phys. Lett.* **89** 252107
[12] Okamoto K, Tada M, Sakamoto T, Miyamura M, Banno N, Iguchi N and Hada H 2011 *IEDM Tech. Dig.* 279
[13] Wang Y F, Qian X Y, Chen K J, Fang Z H, Li W and Xu J 2013 *Appl. Phys. Lett.* **102** 042103
[14] Lian W T, Lv H B, Liu Q, Long S B, Wang W, Wang Y, Li Y T, Zhang S, Dai Y H, Chen J N and Liu M 2011 *IEEE Electron Dev. Lett.* **32** 1053
[15] Salaoru I, Prodromakis T, Khiat A and Toumazou C 2013 *Appl. Phys. Lett.* **102** 013506
[16] Kurnia F, Liu C L, Jung C U and Lee B W 2013 *Appl. Phys. Lett.* **102** 152902
[17] Huang J W, Zhang R, Chang T C, Tsai T M, Chang K C, Lou J C, Young T F, Chen J H, Chen H L, Pan Y C, Huang X, Zhang F Y, Syu Y E and Sze S M 2013 *Appl. Phys. Lett.* **102** 203507
[18] Guan W H, Long S B, Liu Q, Liu M and Wang W 2008 *IEEE Electron Dev. Lett.* **29** 434
[19] Liu Q, Long S B, Wang W, Zuo Q Y, Zhang S, Chen J N and Liu M 2009 *IEEE Electron Dev. Lett.* **30** 1335
[20] Liu Q, Guan W H, Long S B, Jia R and Liu M 2008 *Appl. Phys. Lett.* **92** 012117
[21] Hong S M, Kim H D, An H M and Kim T G 2013 *IEEE Electron Dev. Lett.* **34** 1181
[22] Lin C Y, Wang S Y, Lee D Y and Tseng T Y 2008 *J. Electrochem. Soc.* **155** H615
[23] Choi J S, Kim J S, Hwang I R, Hong S H, Jeon S H, Kang S O, Park B H, Kim D C, Lee M J and Seo S 2009 *Appl. Phys. Lett.* **95** 022109
[24] Xu N, Gao B, Liu L F, Sun B, Liu X Y, Han R Q, Kang J F and Yu B 2008 *Symp. VLSI Tech.* 100
[25] Fan Y S and Liu P T 2014 *IEEE Trans. Electron Dev.* **61** 1071